

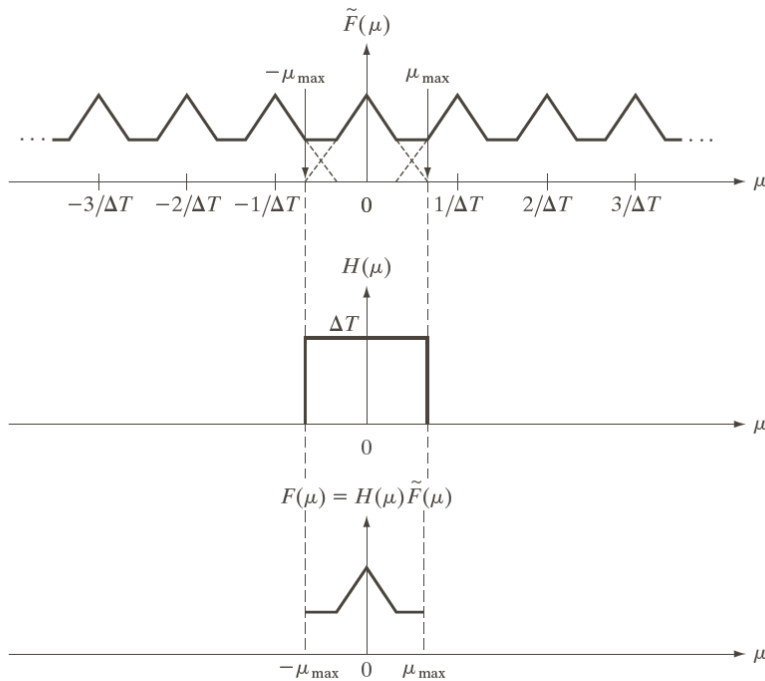
Once we have $F(\mu)$, we can recover $f(t)$ by using the inverse Fourier transform:

$$f(t) = \int_{-\infty}^{\infty} F(\mu)e^{j2\pi\mu t} d\mu . \quad (4.3-9)$$

Equations (4.3-7) through (4.3-9) have proved theoretically that it is possible to recover a **band-limited** function from samples of the function obtained at a rate exceeding twice the highest frequency content of the function. Function $H(\mu)$ is called a **lowpass filter**.

Aliasing

What happens if a **band-limited** function is sampled at a rate that is less than twice its highest frequency? **Figure 4.9** shows the **under-sampled** case.



a
b
c

FIGURE 4.9 (a) Fourier transform of an under-sampled, band-limited function. (Interference from adjacent periods is shown dashed in this figure). (b) The same ideal lowpass filter used in Fig. 4.8(b). (c) The product of (a) and (b). The interference from adjacent periods results in aliasing that prevents perfect recovery of $F(\mu)$ and, therefore, of the original, band-limited continuous function. Compare with Fig. 4.8.

The **inverse transform** would then yield a corrupted function of t . This effect, caused by **under-sampling** a function, is known as **frequency aliasing** or simply as **aliasing**.

Unfortunately, except for some special cases, **aliasing** is always present in sampled signals. Even if the original sampled function is band-limited, infinite frequency components are introduced the moment we limit the duration of the function.

Suppose we want to limit the duration of a **band-limited** function $f(t)$ to an interval $[0, T]$. We can do this by multiplying $f(t)$ by the function

$$h(t) = \begin{cases} 1 & 0 \leq t \leq T \\ 0 & \text{otherwise} \end{cases}, \quad (4.3-10)$$

which has the same basic shape as **Figure 4.4 (a)**.

Recall **Figure 4.4**

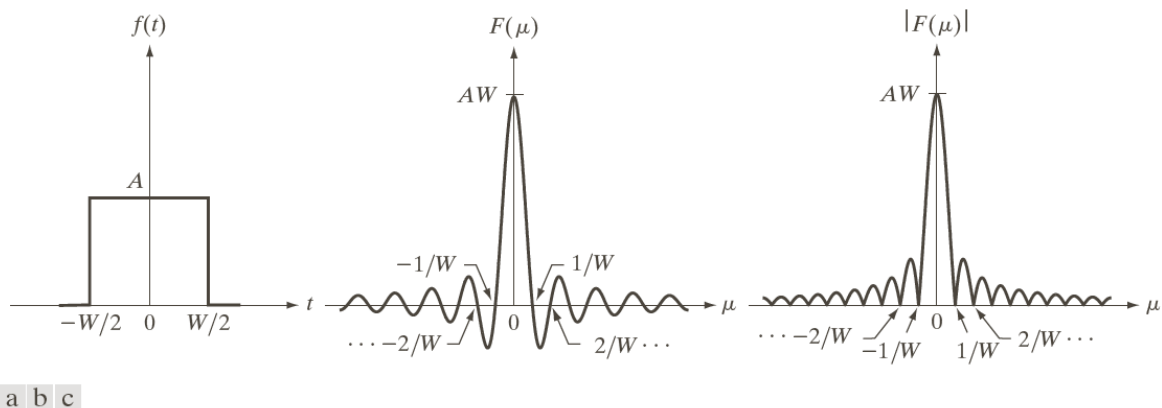


FIGURE 4.4 (a) A simple function; (b) its Fourier transform; and (c) the spectrum. All functions extend to infinity in both directions.

Even if the transform of $f(t)$ is **band-limited**, convolving it with $H(\mu)$, will yield a result with frequency components extending to infinity.

Therefore, no function of finite duration can be band-limited. Conversely, a function that is band-limited must be extended from $-\infty$ to ∞ .

Although **aliasing** is an inevitable fact of working with sampled records of finite length, in practice, the effects of **aliasing** can be reduced by smoothing the input function to attenuate its higher frequencies. This process is called **anti-aliasing**.

The **anti-aliasing** must be done before the function is sampled.

Example 4.3: Aliasing

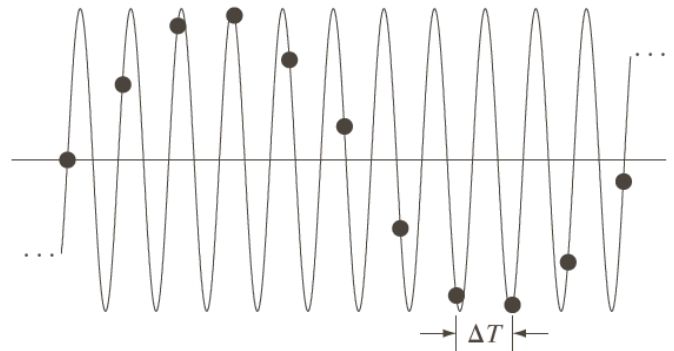


FIGURE 4.10 Illustration of aliasing. The under-sampled function (black dots) looks like a sine wave having a frequency much lower than the frequency of the continuous signal. The period of the sine wave is 2 s, so the zero crossings of the horizontal axis occur every second. ΔT is the separation between samples.

Figure 4.10 shows a classic illustration of aliasing.

Function Reconstruction (Recovery) from Sampled Data

Using the **convolution theorem**, we can obtain the equivalent result in the **spatial domain**. From

$$F(\mu) = H(\mu)\tilde{F}(\mu), \quad (4.3-8)$$

it follows that

$$\begin{aligned} f(t) &= \mathcal{F}^{-1}\{F(\mu)\} \\ &= \mathcal{F}^{-1}\{H(\mu)\tilde{F}(\mu)\} \\ &= h(t) \star \tilde{f}(t). \end{aligned} \quad (4.3-11)$$

It can be shown that substituting (4.3-1) for $\tilde{f}(t)$ into (4.3-11) and using (4.2-20) leads to the following **spatial domain** expression:

$$f(t) = \sum_{n=-\infty}^{\infty} f(n\Delta T)\text{sinc}[(t - n\Delta T)/\Delta T]. \quad (4.3-12)$$

Equation (4.3-12) requires an infinite number of terms for the interpolations between samples.

4.4 Extension to Functions of Two Variables

The 2-D Impulse and Its Sifting Property

The impulse, $\delta(t, z)$, of two continuous variables, t and z , is defined as

$$\delta(t, z) = \begin{cases} \infty & \text{if } t = z = 0 \\ 0 & \text{otherwise} \end{cases} \quad (4.5-1a)$$

and

$$\int_{-\infty}^{\infty} \int_{-\infty}^{\infty} \delta(t, z) dt dz = 1. \quad (4.5-1b)$$

The 2-D impulse exhibits the sifting property under integration

$$\int_{-\infty}^{\infty} \int_{-\infty}^{\infty} f(t, z) \delta(t, z) dt dz = f(0, 0), \quad (4.5-2)$$

or, more generally for an impulse located at (t_0, z_0) ,

$$\int_{-\infty}^{\infty} \int_{-\infty}^{\infty} f(t, z) \delta(t - t_0, z - z_0) dt dz = f(t_0, z_0). \quad (4.5-3)$$

For discrete variables x and y , the 2-D discrete impulse is defined as

$$\delta(x, y) = \begin{cases} 1 & \text{if } x = y = 0 \\ 0 & \text{otherwise} \end{cases} \quad (4.5-4)$$

and its sifting property is

$$\sum_{x=-\infty}^{\infty} \sum_{y=-\infty}^{\infty} f(x, y) \delta(x, y) = f(0, 0). \quad (4.5-5)$$

For an impulse located at (x_0, y_0) , as shown in Figure 4.12, the sifting property is

$$\sum_{x=-\infty}^{\infty} \sum_{y=-\infty}^{\infty} f(x, y) \delta(x - x_0, y - y_0) = f(x_0, y_0). \quad (4.5-6)$$

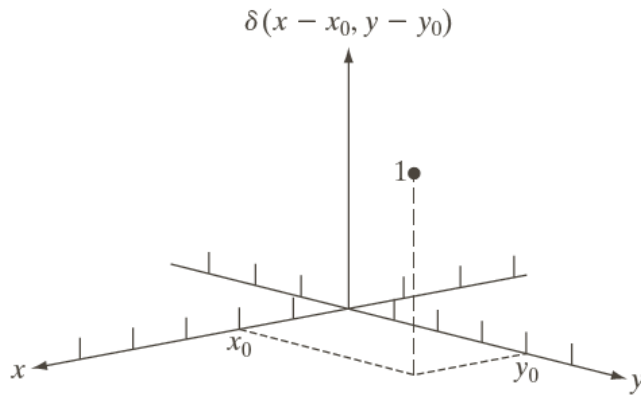


FIGURE 4.12
Two-dimensional unit discrete impulse. Variables x and y are discrete, and δ is zero everywhere except at coordinates (x_0, y_0) .

The 2-D Continuous Fourier Transform Pair

Let $f(t, z)$ be a continuous function of two continuous variables. The 2-D continuous Fourier transform pair is given by the expressions

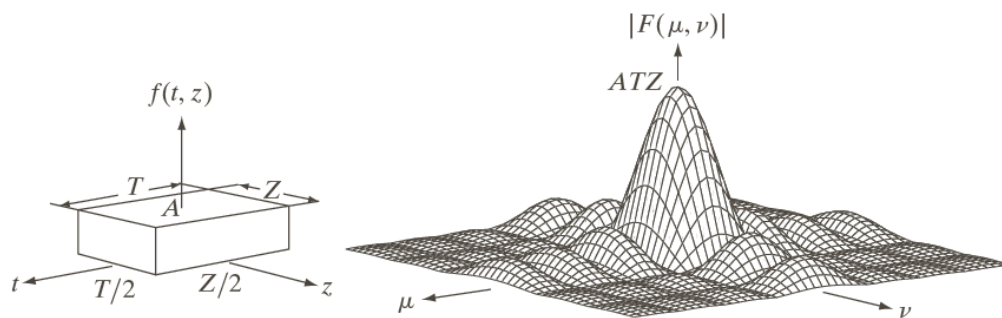
$$F(\mu, \nu) = \int_{-\infty}^{\infty} \int_{-\infty}^{\infty} f(t, z) e^{-j2\pi(\mu t + \nu z)} dt dz \quad (4.5-7)$$

and

$$f(t, z) = \int_{-\infty}^{\infty} \int_{-\infty}^{\infty} F(\mu, \nu) e^{j2\pi(\mu t + \nu z)} d\mu d\nu \quad (4.5-8)$$

where μ and ν are the frequency variables.

Example 4.5: Obtaining the 2-D Fourier transform of a simple function



a b

FIGURE 4.13 (a) A 2-D function, and (b) a section of its spectrum (not to scale). The block is longer along the t -axis, so the spectrum is more “contracted” along the μ -axis. Compare with Fig. 4.4.

$$\begin{aligned} F(\mu, \nu) &= \int_{-\infty}^{\infty} \int_{-\infty}^{\infty} f(t, z) e^{-j2\pi(\mu t + \nu z)} dt dz \\ &= \int_{-T/2}^{T/2} \int_{-Z/2}^{Z/2} A e^{-j2\pi(\mu t + \nu z)} dt dz \\ &= ATZ \left[\frac{\sin(\pi\mu T)}{(\pi\mu T)} \right] \left[\frac{\sin(\pi\nu Z)}{(\pi\nu Z)} \right] \end{aligned}$$

The **magnitude** is given by the expression

$$|F(\mu, \nu)| = ATZ \left| \frac{\sin(\pi\mu T)}{(\pi\mu T)} \right| \left| \frac{\sin(\pi\nu Z)}{(\pi\nu Z)} \right|$$

Two-Dimensional Sampling and Sampling Theorem

Sampling in 2-D can be modeled using the **sampling function** (2-D impulse train):

$$s_{\Delta T \Delta Z}(t, z) = \sum_{m=-\infty}^{\infty} \sum_{n=-\infty}^{\infty} \delta(t - m\Delta T, z - n\Delta Z) \quad (4.5-9)$$

where ΔT and ΔZ are the separations between samples along the t -axis and z -axis. Equation (4.5-9) describes a set of the **periodic impulses** extending along the two axes, as shown in Figure 4.14.

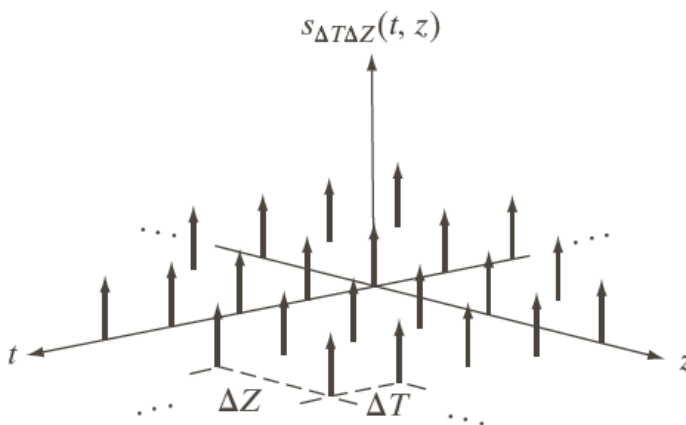


FIGURE 4.14
Two-dimensional impulse train.

Function $f(t, z)$ is said to be **band-limited** if its **Fourier transform** is 0 outside a rectangle established by the intervals $[-\mu_{\max}, \mu_{\max}]$ and $[-\nu_{\max}, \nu_{\max}]$:

$$F(\mu, \nu) = 0 \quad \text{for } |\mu| \geq \mu_{\max} \quad \text{and} \quad |\nu| \geq \nu_{\max} \quad (4.5-10)$$

The **two-dimensional sampling theorem** states that a continuous, **band-limited** function $f(t, z)$ can be recovered with no error from a set of its samples if the **sampling intervals** are

$$\Delta T < \frac{1}{2\mu_{\max}} \quad (4.5-11)$$

and

$$\Delta Z < \frac{1}{2\nu_{\max}}, \quad (4.5-12)$$

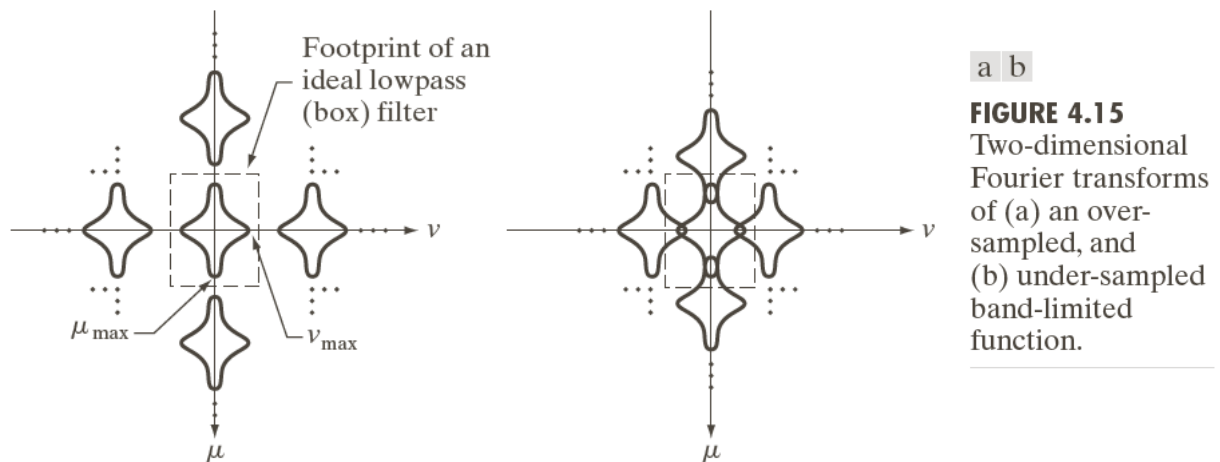
or expressed in terms of the sampling rate, if

$$\frac{1}{\Delta T} > 2\mu_{\max} \quad (4.5-13)$$

and

$$\frac{1}{\Delta Z} > 2\nu_{\max}. \quad (4.5-14)$$

Figure 4.15 shows the 2-D equivalents of Figure 4.6 (b) and (d).



The dashed portion of Figure 4.15 (a) shows the location of an **ideal box filter**, as shown in Figure 4.13 (a), to achieve the necessary **isolation** of a single period of the transform for reconstruction of a **band-limited function** from its samples.

Aliasing in Images

Extension from 1-D aliasing

As in the 1-D case, $f(t, z)$ can be **band-limited** in general only if it extends infinitely in both coordinates directions. So, **aliasing** is always present in digital images.

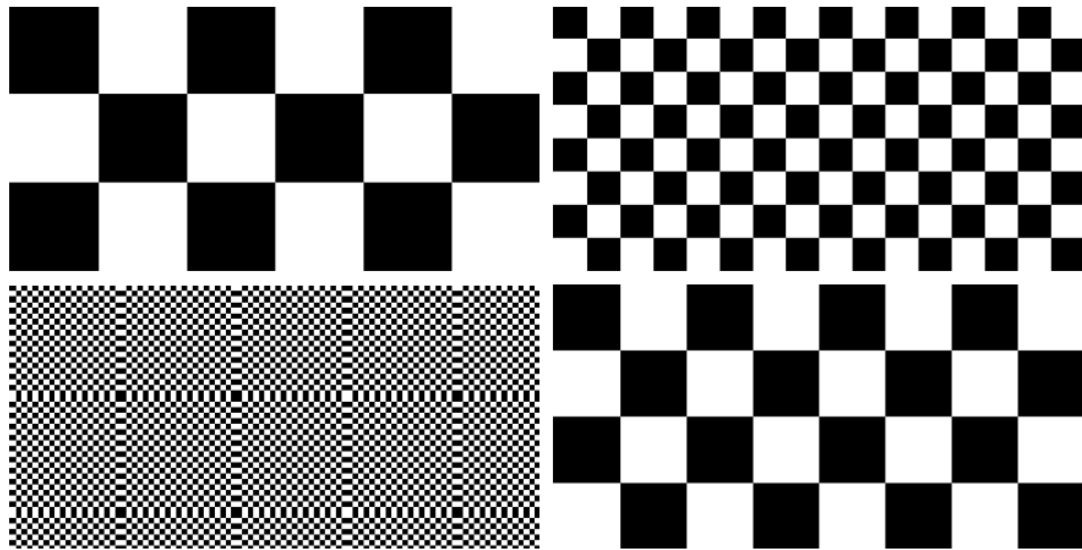
There are two principal manifestations of **aliasing** in images: **spatial aliasing**, which is due to **under-sampling**; and **temporal aliasing**, which is related to time intervals between images in a sequence of images.

Example 4.6: Aliasing in images

Assume that we have a perfect imaging system that is noiseless and produces an exact digital image of what it sees, but the number of samples it can take is fixed at 96×96 pixels.

If we use this system to digitize checkerboard patterns, it will be able to resolve patterns that are up to 96×96 squares, in which the size of each square is 1×1 pixels.

We are interested in examining what happens when the imaging system is asked to digitize checkerboard patterns that have more than 96×96 squares in the field of view.



a b
c d

FIGURE 4.16 Aliasing in images. In (a) and (b), the lengths of the sides of the squares are 16 and 6 pixels, respectively, and aliasing is visually negligible. In (c) and (d), the sides of the squares are 0.9174 and 0.4798 pixels, respectively, and the results show significant aliasing. Note that (d) masquerades as a “normal” image.

When the size of the squares is reduced to slightly less than one camera pixel, the system produce a severely aliased image, as [Figure 4.16 \(c\)](#) shows.

When the size of the squares is reduced to slightly less than half of a camera pixel, the system will produce a severely aliased and image, which is very misleading, as [Figure 4.16 \(d\)](#) shows.

The effects of [aliasing](#) can be reduced by slightly [defocusing](#) the scene to be digitized so that high frequencies are attenuated.

The [anti-aliasing filtering](#) has to be done at the “[front-end](#)”, before the image is sampled. There are no such things as [after-the-fact](#) software [anti-aliasing filters](#) that can be used to reduce the effects of [aliasing](#) caused by violations of the [sampling theorem](#).

Image interpolation and resampling

As in the 1-D case, perfect reconstruction of a **band-limited** image function from a set of its samples requires **2-D convolution** in the **spatial domain** with a **sinc** function.

As mentioned previously, this theoretically perfect reconstruction requires interpolation using infinite summations. Therefore, in practice, we need to look for approximations.

One of the most common applications of **2-D interpolation** in image processing is in image **resizing** (**zooming** and **shrinking**).

A special case of **nearest neighbour interpolation** that ties with **over-sampling** is zooming by pixel replication, which is applicable when we want to **increase** the size of an image by an integer number of times.

For example, to double the size of an image, we duplicate each column, and then each row of the enlarged image. The intensity-level assignment of each pixel is predetermined by the fact that new locations are exact duplicates of old locations.

Image shrinking is done in a similar manner. **Under-sampling** is achieved by row-column deletion.

Example 4.7: Illustration of aliasing in resampled images

The effects of **aliasing** generally are worsened when the size of a digital image is reduced.



a b c

FIGURE 4.17 Illustration of aliasing on resampled images. (a) A digital image with negligible visual aliasing. (b) Result of resizing the image to 50% of its original size by pixel deletion. Aliasing is clearly visible. (c) Result of blurring the image in (a) with a 3×3 averaging filter prior to resizing. The image is slightly more blurred than (b), but aliasing is not longer objectionable. (Original image courtesy of the Signal Compression Laboratory, University of California, Santa Barbara.)

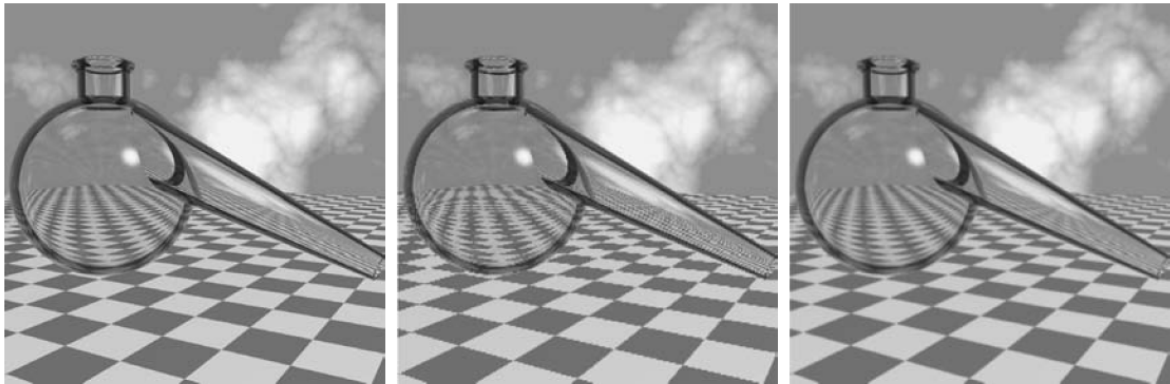
Figure 4.17 (a) is an image purposely created to show the effects of **aliasing**. Although there are the thinly-spaced parallel lines in all garments worn, there are no objectionable artifacts in **Figure 4.17 (a)**, indicating that the sampling rate was sufficient to avoid visible **aliasing**.

In **Figure 4.17 (b)**, the image was reduced to **50%** of its original size using row-column deletion. The effects of **aliasing** are quite visible.

Figure 4.17 (c) shows the result of smoothing the image in **Figure 4.17 (a)** is a 3×3 averaging filter before reducing its size. The improvement over **Figure 4.17 (a)** is evident.

When we work with images that have strong **edge content**, the effects of **aliasing** are seen as **block-like** image components, called **jaggies**.

Example 4.8: Illustration of jaggies in image shrinking



a b c

FIGURE 4.18 Illustration of jaggies. (a) A 1024×1024 digital image of a computer-generated scene with negligible visible aliasing. (b) Result of reducing (a) to 25% of its original size using bilinear interpolation. (c) Result of blurring the image in (a) with a 5×5 averaging filter prior to resizing it to 25% using bilinear interpolation. (Original image courtesy of D. P. Mitchell, Mental Landscape, LLC.)

Figure 4.18 (a) shows a 1024×1024 image of a computer-generated scene in which **aliasing** is negligible.

Figure 4.18 (b) is the result of reducing the size by 75% to 256×256 using **bilinear interpolation** and then using pixel replication to bring the image back to its original size in order to make the effects of **aliasing** more visible.

Figure 4.18 (c) is the result of using a 5×5 averaging filter prior to reducing the size of image. Compared to **Figure 4.18 (b)**, **jaggies** in **Figure 4.18 (c)** were reduced significantly.

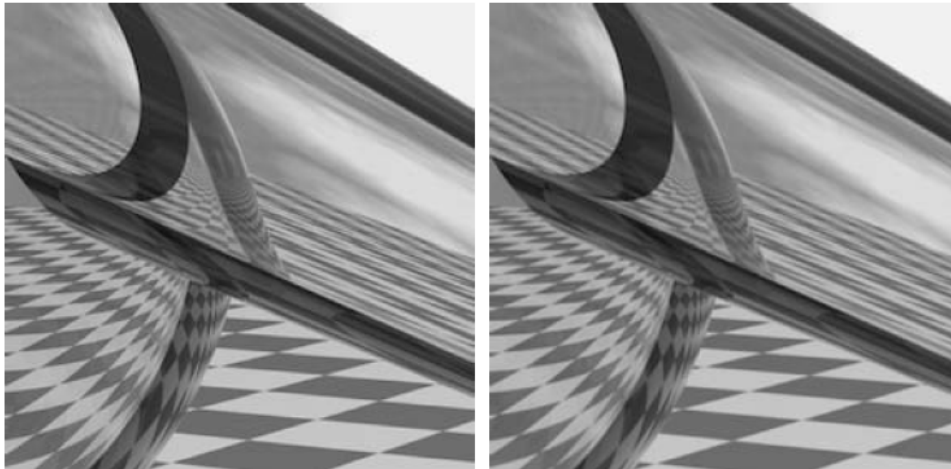
Example 4.9: Illustration of jaggies in image zooming

Figure 4.19 (a) shows a 1024×1024 zoomed image generated by pixel replication from a 256×256 section out of the center of Figure 4.18 (a).

Note the “blocky” edges in Figure 4.19 (a).

The zoomed image in Figure 4.19 (b) was generated from the same 256×256 section, but using bilinear interpolation.

The edges in Figure 4.19 (b) are considerably smooth.



a b

FIGURE 4.19 Image zooming. (a) A 1024×1024 digital image generated by pixel replication from a 256×256 image extracted from the middle of Fig. 4.18(a). (b) Image generated using bi-linear interpolation, showing a significant reduction in jaggies.

4.5 The Discrete Fourier Transform (DFT) of One Variable

The material up to this point may be viewed as the foundation of introducing the **discrete Fourier transform (DFT)**, which is the main part of **Chapter 4**.

Obtaining the DFT from the Continuous Transform of a Sampled Function

Referring to

$$F(\mu) = \int_{-\infty}^{\infty} f(t)e^{-j2\pi\mu t} dt \quad (4.2-16)$$

and by substituting

$$\tilde{f}(t) = \sum_{n=-\infty}^{\infty} f(t)\delta(t - n\Delta T) \quad (4.3-1)$$

for $\tilde{f}(t)$, we obtain

$$\begin{aligned} \tilde{F}(\mu) &= \int_{-\infty}^{\infty} \tilde{f}(t)e^{-j2\pi\mu t} dt \quad (4.4-1) \\ &= \int_{-\infty}^{\infty} \sum_{n=-\infty}^{\infty} f(t)\delta(t - n\Delta T)e^{-j2\pi\mu t} dt \\ &= \sum_{-\infty}^{\infty} \int_{-\infty}^{\infty} f(t)\delta(t - n\Delta T)e^{-j2\pi\mu t} dt \\ &= \sum_{-\infty}^{\infty} f_n e^{-j2\pi\mu n\Delta T} \quad (4.4-2) \end{aligned}$$

Although f_n is a **discrete function**, its Fourier $\tilde{F}(\mu)$ is **continuous** and **infinitely periodic** with period $1/\Delta T$. Therefore, all we need to characterize $\tilde{F}(\mu)$ is one period, and **sampling one period** is the basis for the **DFT**.

Suppose that we want to have M equally spaced samples of $\tilde{F}(\mu)$ over the period $\mu = 0$ to $\mu = 1/\Delta T$, we will take the samples at the frequencies

$$\mu = \frac{m}{M\Delta T} \quad m = 0, 1, 2, \dots, M - 1 \quad (4.4-3)$$

Substituting into (4.4-2) and using F_m to denote the result

$$F_m = \sum_{n=0}^{M-1} f_n e^{-j2\pi mn/M} \quad m = 0, 1, 2, \dots, M - 1 \quad (4.4-4)$$

This is the **discrete Fourier transform** we are seeking.

Conversely, given $\{F_m\}$, we can recover the sample set $\{f_n\}$ by using the **inverse discrete Fourier transform (IDFT)**

$$f_n = \frac{1}{M} \sum_{m=0}^{M-1} F_m e^{j2\pi mn/M} \quad n = 0, 1, 2, \dots, M - 1 \quad (4.4-5)$$

Equations (4.4-4) and (4.4-5) constitute a **discrete Fourier transform pair**.

The **forward** and **inverse Fourier transforms** exist for any set of samples whose values are finite.

Note that neither expression depends on the sampling interval ΔT nor on the frequency intervals of μ . Therefore, the **DFT pair** is applicable to any finite set of discrete samples taken uniformly.

For image processing, we intend to use the notation x and y for image coordinates variables and u and v for frequency variables.

Then, (4.4-4) and (4.4-5) become

$$F(u) = \sum_{n=0}^{M-1} f(x)e^{-j2\pi ux/M} \quad u = 0, 1, 2, \dots, M-1 \quad (4.4-6)$$

and

$$f(x) = \frac{1}{M} \sum_{u=0}^{M-1} F(u)e^{j2\pi ux/M} \quad x = 0, 1, 2, \dots, M-1. \quad (4.4-7)$$

It can be shown that both the forward and inverse discrete transforms are infinitely periodic, with period M ,

$$F(u) = F(u + kM) \quad (4.4-8)$$

and

$$f(x) = f(x + kM) \quad (4.4-9)$$

where k is an integer.

The discrete equivalent of convolution in

$$f(t) \star h(t) = \int_{-\infty}^{\infty} f(\tau)h(t - \tau)d\tau \quad (4.2-20)$$

is

$$f(x) \star h(x) = \sum_{m=0}^{M-1} f(m)h(x - m) \quad (4.4-10)$$

for $x = 0, 1, 2, \dots, M-1$.

Equation (4.4-10) gives one period of the periodic convolution, therefore, the process is referred to as circular convolution and is a direct result of the periodicity of the DFT and its inverse.

Relationship between the Sampling and Frequency Intervals

If $f(x)$ consists of M samples of a function $f(t)$ taken ΔT units apart, the duration is

$$T = M\Delta T. \quad (4.4-11)$$

In the discrete frequency domain, the corresponding spacing, $\Delta\mu$, is

$$\Delta\mu = \frac{1}{M\Delta T} = \frac{1}{T}. \quad (4.4-12)$$

The entire frequency range spanned by the M components of the DFT is

$$\Omega = M\Delta\mu = \frac{1}{\Delta T}. \quad (4.4-13)$$

The resolution in frequency, $\Delta\mu$, of the DFT depends on the duration T over which the continuous function, $f(t)$, is sampled. The range of frequencies spanned by the DFT depends on the sampling interval ΔT .

Example 4.4: The mechanics of computing the DFT

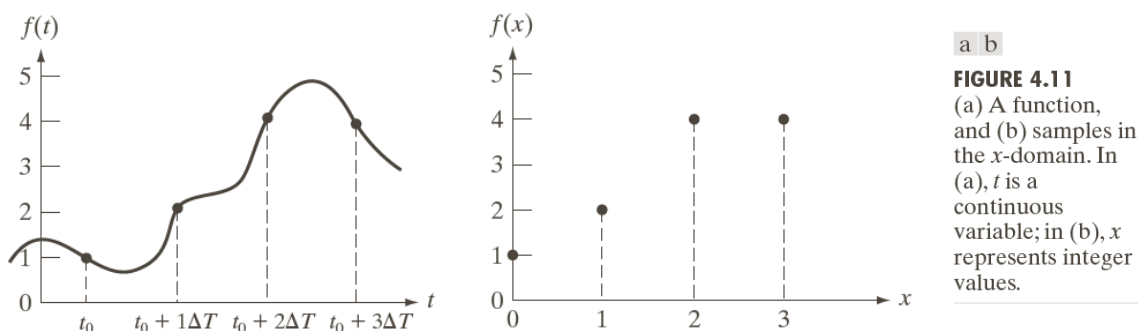


FIGURE 4.11
(a) A function, and (b) samples in the x -domain. In (a), t is a continuous variable; in (b), x represents integer values.

Figure 4.11 (a) shows four samples of a continuous function $f(t)$, and Figure 4.11 (b) shows the sampled values in the x -domain.

From

$$F(u) = \sum_{n=0}^{M-1} f(x)e^{-j2\pi ux/M} \quad u = 0,1,2,\dots,M-1, \quad (4.4-6)$$

we obtain

$$\begin{aligned} F(0) &= \sum_{x=0}^3 f(x) = [f(0) + f(1) + f(2) + f(3)] \\ &= 1 + 2 + 4 + 4 = 11, \end{aligned}$$

and the next value of $F(u)$

$$\begin{aligned} F(1) &= \sum_{x=0}^3 f(x)e^{-j2\pi(1)x/4} \\ &= 1e^0 + 2e^{-j\pi/2} + 4e^{-j\pi} + 4e^{-j3\pi/2} = -3 + 2j \end{aligned}$$

Similarly, we have $F(2) = -(1 + 0j)$ and $F(3) = -(3 + 2j)$.

If we were given $F(u)$ and were asked to compute its **inverse**, we would use the **inverse transform**

$$f(x) = \frac{1}{M} \sum_{u=0}^{M-1} F(u)e^{j2\pi ux/M} \quad x = 0,1,2,\dots,M-1. \quad (4.4-7)$$

For example,

$$\begin{aligned} f(0) &= \frac{1}{4} \sum_{u=0}^3 F(u)e^{j2\pi u(0)} = \frac{1}{4} \sum_{u=0}^3 F(u) \\ &= \frac{1}{4}[11 - 3 + 2j - 1 - 3 - 2j] = 1 \end{aligned}$$

The 2-D Discrete Fourier Transform and Its Inverse

The 2-D discrete Fourier transform (DFT) is

$$F(u, v) = \sum_{x=0}^{M-1} \sum_{y=0}^{N-1} f(x, y) e^{-j2\pi(ux/M + vy/N)}, \quad (4.5-15)$$

for $u = 0, 1, 2, \dots, M - 1$ and $v = 0, 1, 2, \dots, N - 1$.

Given $F(u, v)$, we can obtain $f(x, y)$ by using the inverse discrete Fourier transform (IDFT):

$$f(x, y) = \frac{1}{MN} \sum_{u=0}^{M-1} \sum_{v=0}^{N-1} F(u, v) e^{j2\pi(ux/M + vy/N)}, \quad (4.5-16)$$

for $x = 0, 1, 2, \dots, M - 1$ and $y = 0, 1, 2, \dots, N - 1$.

Equations (4.5-15) and (4.5-16) constitute the 2-D discrete Fourier transform pair.